Nuclear Instruments and Methods 195 (1982) 475–482
North-Holland Publishing Company

CHARACTERISTICS OF LEAD–SCINTILLATOR SAMPLING SHOWER COUNTERS FOR THE DETECTION OF ELECTRONS AND PHOTONS IN THE ENERGY RANGE 70 MeV TO 6 GeV

W. HOFMANN, A. MARKEES, U. MATTHIESEN, O. MÄDIGER, M. SCHMELLING and D. WEGENER

Institut für Physik, Universität Dortmund, Fed. Rep. Germany

Received 11 September 1981

A lead–scintillator shower counter using fluorescent radiation converters to collect scintillation light was tested with electrons and photons in the energy range 70 MeV to 6 GeV. The influence of the various design parameters was investigated. Typical resolutions obtained were $\sigma \simeq 7\%/E^{1/2}$ (in GeV) for photon or electron energies, and $\sigma_x \simeq 11$ mm$/E^{1/2}$ (in GeV) for the impact position.

1. Introduction

The use of sampling shower counters is a well established technique for the measurement of the energies of electrons or photons. A sampling shower counter consists of alternate layers of absorber material (typically lead or iron) and of detector material (e.g. scintillator). The total energy of an electromagnetic shower contained in the calorimeter is estimated from the fraction of energy deposited in the detection layers. The performance of a calorimeter, i.e. its energy resolution and its ability to reconstruct the impact point of a particle depends on the number of sampling steps, and on the spatial segmentation of the detection layers, respectively. In the case of lead–scintillator calorimeters, the introduction of fluorescent radiation converters [1] for the collection of scintillation light made it possible to combine both fine-grained sampling and extensive segmentation [2,3].

In an earlier paper [3], we reported on the first tests of such a shower counter system, which will be used in the solenoid detector ARGUS at DORIS.

In this work, we describe further and more detailed studies of this modular system of shower counters. The paper is subdivided as follows: in section 2, the design of the counter modules is briefly reviewed. Several different absorber configurations have been measured in order to study the influence of the design parameters, like the thickness of the lead plates, the choice of the scintillator material, etc. The results are discussed in section 3. Finally, the performance of the counter system used to detect and localize electrons and photons in the energy range 70 MeV to 6 GeV is summarized in section 4.

2. Calorimeter modules

As in previous tests [3], the setup consisted of several identical calorimeter modules arranged in a matrix. Each module contained alternate layers of plastic scintillator and lead plates. In the so-called "standard configuration", the thickness of the lead plates was 1 mm, as compared with the 5 mm thickness of the scintillator layers. The active front area of one module was 10×10 cm^2; the depth of the absorber stack was fixed at 40 cm, corresponding to ~ 12.5 radiation lengths.

One side of the lead/scintillator stack was covered by a sheet of wavelength shifting plastic. The blue light

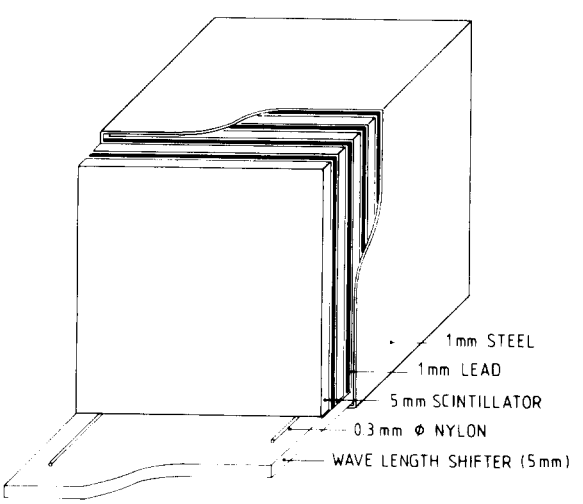

Fig. 1. Schematic view of one of the test modules.

0029-554X/82/0000–0000/$02.75

Table 1
"Standard" calorimeter module

Absorber	$10\times10\times0.1$ cm^3 lead plates, alternating with $10\times10\times0.5$ cm^3 scintillator plates Plexipop GS 1922 [a] (3% Napthalene, 1% butyl PBD, 0.01% POPOP), with polished edges, wrapped into aluminium foil; total depth of absorber stack: 40 cm; mean density: 2.9 g/cm^3; mean radiation length 3.1 cm.
Readout	$0.5\times10\times40$ cm^3 wave-length shifter bar, Plexiglas GS 218 [a] (120 mg BBQ/l), backed with aluminium foil; adiabatic light guide; Photomultiplier XP 2008 UB [b]
Dimensions of module including steel housing and light guide:	$10.3\times10.8\times80$ cm
Active front area:	90%

[a] Röhm GmbH, Darmstadt, FRG.
[b] Valvo, Hamburg, FRG.

from the scintillator traverses a small air gap, enters the wavelength-shifter bar, and is converted into green fluorescence light, part of which is trapped in the shifter bar and, via an adiabatic light guide, is transported to a 1″ photomultiplier. Two 0.3 mm nylon threads between the wavelength shifter and the absorber plates serve to maintain the air gap, which is required in order not to disturb the total reflection of light trapped in the wavelength shifter.

The whole assembly was put into a 1 mm steel housing. A schematic view of one module is given in fig. 1; further details are listed in table 1.

Several counter modules were arranged in a matrix and were tested in a tagged photon beam, at energies ranging from ~70 to ~380 MeV. Data at higher energies, up to 6 GeV, were obtained in an electron beam. In each case, the momentum spread and the spatial width of the beams was negligible as compared with the resolution of the calorimeter array.

3. Choice of design parameters

According to the physics aims of the ARGUS-experiment, the shower counters were optimized for the detection of photons of a few tens up to a few hundred MeV; the maximum photon energy is ~5 GeV.

The energy resolution of sampling shower counter is determined by three components:

(i) due to leakage, mainly at the rear end, the total amount of energy deposited in the shower counter may fluctuate. An estimate of the energy spread E_L due to rear leakage is given by

$$\delta E_l \simeq \delta t\,(\mathrm{d}E/\mathrm{d}t)_{t_0}, \tag{1}$$

where $(\mathrm{d}E/\mathrm{d}t)_{t_0}$ is the average energy deposited per radiation length λ_{rad} at the rear end t_0 of the counter, and δt is the r.m.s. fluctuation of the shower center within the absorber in units of λ_{rad}. Since δt is mainly determined by the position of the first interaction of an incoming photon with matter, we expect δt to be of the order of 1 radiation length. Using a standard parametrisation for $(\mathrm{d}E/\mathrm{d}t)$ [4]

$$(\mathrm{d}E/\mathrm{d}t) \simeq E_0 A t^{\alpha} \mathrm{e}^{-\beta t} \tag{2}$$

and ignoring the small (logarithmic) variation of α and β with the photon energy E_0, we obtain for energies of 0 (1 GeV) [4]

$$(\mathrm{d}E/\mathrm{d}t) \simeq E_0 \gamma t^2 \mathrm{e}^{-t/2} \tag{3}$$

with $\gamma \simeq 0.063$, or

$$\sigma_L = (\delta E_L/E_0) \simeq \gamma t_0^2 \mathrm{e}^{-t_0/2}. \tag{4}$$

(ii) Fluctuation of the fraction of energy deposited in the scintillator. These "sampling fluctuations" depend on the size τ of one sampling step, i.e. the thickness of one lead–scintillator cell measured in units of λ_{rad}. The amount of these sampling fluctuations can be estimated by noting that the total track length L (in units of λ_{rad}) of particles in the shower,

$$L \simeq E_0/\epsilon, \tag{5}$$

where ϵ is the critical energy, is sampled in steps of τ, yielding $N = (E_0/\epsilon\tau)$ crossings of particles through detection layers. The relative r.m.s. fluctuation of the energy seen in the scintillator is then

$$\sigma_S = \delta E_{\mathrm{scint}}/E_{\mathrm{scint}} \simeq N^{-1/2} = (\tau\epsilon/E_0)^{1/2}. \tag{6}$$

Corrections to eq. (6) [9], which arise as a result of low-energy threshold effects and due to the path-length straggling of the shower particles are small and can be neglected in the present case.

(iii) "Noise" or fluctuations of the signals from the detection layers. The most stringent limitation is due to the finite number of photoelectrons in the PM, yielding

$$\sigma_N = \delta E_N/E_0 \simeq (E_0 \bar{n})^{-1/2}, \tag{7}$$

where $\bar{n}$ is the mean number of photoelectrons per unit incident energy.

Combining eqs. (4), (6), (7), we obtain for the relative energy resolution

$$\sigma = \delta E/E_0 \simeq \left(\gamma^2 t_0^4 \mathrm{e}^{-t_0} + \frac{\tau\epsilon}{E_0} + \frac{1}{E_0\bar{n}}\right)^{1/2}, \tag{8}$$

or, in terms of the normalized resolution

$$\sigma_0 = \sigma E_0^{1/2} \simeq \left(E_0\gamma^2 t_0^4 \mathrm{e}^{-t_0} + \tau\epsilon + \frac{1}{\bar{n}}\right)^{1/2}. \tag{9}$$

σ_0 is energy independent provided that leakage is negligible; at large energies, however, the leakage term dominates.

Using eq. (9), we can further estimate the position resolution of an array of calorimeter modules. Consider a row of counters, and denote by $x = 0$ the position of the center of the module, which is hit by an incident photon. The impact position x_0 within the center module n can be calculated from the leakage into the neighboured modules $n-1$ and $n+1$ centered at $x = +A$ and $x = -A$, respectively.

Define the center of gravity of a shower as

$$\tilde{x} = \frac{\sum E_i(x)\, x_i}{\sum E_i} \simeq \frac{A[E_{n+1}(x) - E_{n-1}(x)]}{E_0} \tag{10}$$

the position resolution for the x-coordinate is in the worst case ($x \simeq 0$)

$$\delta x = \left(\frac{\mathrm{d}x}{\mathrm{d}\tilde{x}}\right)\Big|_{\tilde{x}\simeq 0} \delta\tilde{x} = \left(\frac{\mathrm{d}x}{\mathrm{d}\tilde{x}}\right)\Big|_{\tilde{x}\simeq 0} \left[\sum \left(\frac{\partial\tilde{x}}{\partial E_i}\delta E_i\right)^2\right]^{1/2} \tag{11}$$

At typical energies, the amount of shower energy leaking through a boundary at a distance y from the shower axis into a neighbouring module can be approximated by [3]

$$E_L = \frac{E_0}{2}\, \mathrm{e}^{-y/a_0}, \tag{12}$$

with $a_0 \simeq 2$ cm. Assuming that the fluctuation of E_L is given by eqs. (6) and (7), we find

$$\delta x \simeq \frac{a_0\sigma_0}{E_0^{1/2}}\, \mathrm{e}^{A/4a_0}. \tag{13}$$

In reality, δx will be somewhat larger, since due to correlations the fluctuation of E_L is increased as compared with eq. (6).

The design criteria for the counter modules are now obvious: the energy resolution at low energies is determined mainly by the thickness of the lead plates, $\tau \simeq \tau_{\mathrm{lead}}$, provided that the scintillator thickness is chosen such that photoelectron statistics does not limit the energy resolution.

As a compromise between the size of the counters and the influence of leakage, t_0 should be chosen such that at the highest energy the terms in eqs. (4) and (6) are of the same order of magnitude.

For the standard configuration (table 1) the various terms contributing to eq. (9) are of the following order of magnitude:

Sampling fluctuations $\sigma E^{1/2} =$	$5\%\mathrm{GeV}^{1/2}$
Photoelectron statistics (estimated using the known efficiencies for light collection, conversion, and transport to the photocathode [1])	$3\text{–}4\%\mathrm{GeV}^{1/2}$
Leakage fluctuations:	
at $E_0 \simeq 1$ GeV	2%
at $E_0 \simeq 5$ GeV	5%

(14)

yielding $\sigma_0 \simeq 6 \ldots 7\%\ \mathrm{GeV}^{1/2}$ at low energies, and $\sigma_0 \simeq 8\%$ at $E_0 \simeq 5$ GeV.

For the position resolution in each projection we expect that

$$\delta x \simeq b/E_0^{1/2}, \tag{15}$$

with b of the order 0.5 cm. Various experimental tests have been performed in order to systematically study the terms contributing to eq. (9).

In a first series of measurements, the thickness of the lead plates D, and correspondingly of the scintillator plates was varied between 0.5 to 16 mm, and 2.5 to 80 mm, respectively, with the aim of studying the contribution due to sampling fluctuations. Scintillator plates of 10 mm, 20 mm etc thickness were obtained by adding 2, 4 etc 5 mm scintillator sheets, each of which was wrapped separately in aluminium foil. This procedure guarantees that conditions of light collection remain unchanged over the whole series.

Fig. 2 shows the normalized energy resolution σ_0, averaged over measurements with incident photons of

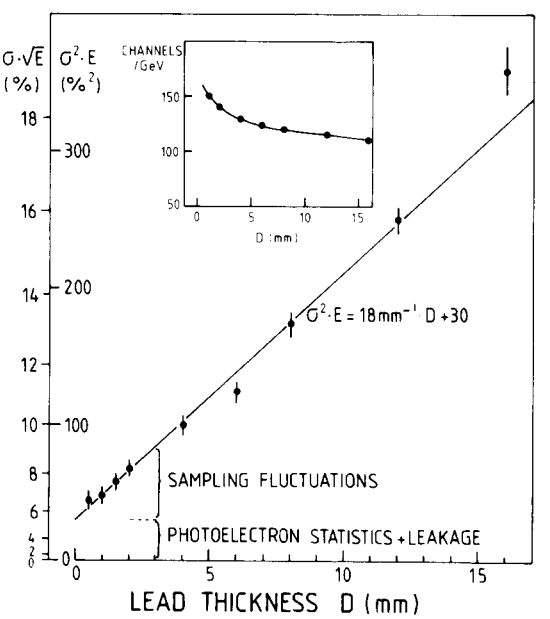

Fig. 2. Normalized energy resolution $\sigma E^{1/2}$ (E in GeV) as a function of the thickness D of the lead absorber-plates, obtained with photons at energies between 200 MeV and 320 MeV. The thickness of scintillator layers is $5D$. The full curve is a fit to the data points, $\sigma^2 E = sD + s_0$, with $s = 18\ \mathrm{mm}^{-1}$ and $s_0 = 30$, for σ in percent and E in GeV. Insert: mean pulse height, normalized to 1 GeV photons, as a function of D.

200, 260 and 320 MeV. At these energies leakage at the rear end of the module is negligible; however since these tests were carried out with a single module not imbedded into a matrix of counters, some leakage at the sides will have occurred.

From eq. (9), we expect a linear relationship between the plate thickness D and the resolution squared σ_0^2.

Fig. 2 demonstrates that σ_0^2 does grow linearly with D. The observed slope $s = 18\ \text{mm}^{-1}$ (for σ in per cent and E in GeV) is compatible with the value $23\ \text{mm}^{-1}$ estimated on the basis of eq. (9). From the extrapolation to $D = 0$, the sum of the leakage- and photostatistics-terms is determined to be 5.5% $\text{GeV}^{1/2}$. From calibration runs with light emitting diodes, the contribution of photoelectron statistics alone was determined to be $\sim$ 3.7% $\text{GeV}^{1/2}$, corresponding to an effective number of $\sim$ 700–800 photoelectrons per GeV incident energy (for the standard configuration described in table 1).

It is interesting to note that the fraction of energy visible in the scintillator decreases with increasing thickness of the lead plates (small insert in fig. 2). This behaviour arises due to transition effects [5,6] at the lead–scintillator boundaries: in the rear part of an electromagnetic shower, energy flux is maintained mainly by low-energy photons [6,7], and energy is deposited by slow electrons arising from conversions of these photons. In an homogeneous material, the ratio of the numbers of electrons and photons reaches an equilibrium value [6], which is larger in lead, as compared with the scintillator. If the sampling τ is small compared with the range of these low-energy electrons, the absorber essentially acts as an homogeneous medium. For larger τ however, the number of shower electrons in the scintillator decreases as compared with the lead plates, and the visible energy diminishes.

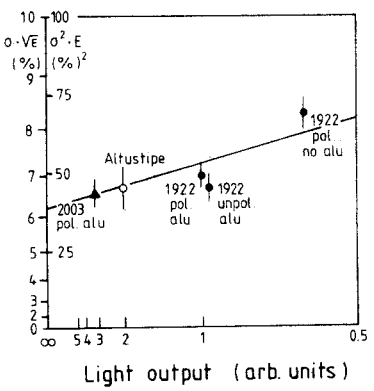

Fig. 3. Normalized energy resolution $\sigma E^{1/2}$ (E in GeV) versus mean light output for different scintillator types (Plexiglass 1922, 2003; Altustipe); for polished and unpolished edges of the scintillator plates, and with or without wrapping in aluminium foil. The slope of the full line is calculated using the known mean number of photoelectrons per unit light output.

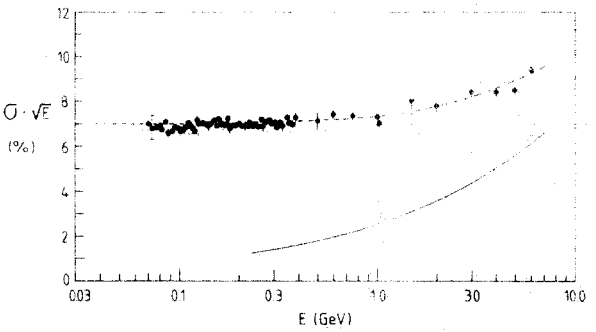

Fig. 4. Normalized energy resolution $\sigma E^{1/2}$ (E in GeV) as a function of energy. Full error bars refer to statistical errors; the dotted bars indicate systematic uncertainties at low energies. The full line shows the limitation due to leakage, the dotted line is a quadratic sum of leakage terms plus a constant.

In order to investigate the influence of light collection and photoelectron statistics in more detail, several types of scintillator material were used. In the standard configuration, 1 mm lead/5 mm scintillator, the following combinations were tested:

Scintillator Plexipop 1922 *, polished edges, wrapped into aluminium foil;

Scintillator Plexipop 1922 *, rough unpolished edges, wrapped into aluminium foil;

Scintillator Plexipop 1922 *, polished edges, no aluminium foil;

Scintillator Plexipop 2003 *, polished edges, wrapped into aluminium foil;

Scintillator Altustipe **, polished edges, wrapped into aluminium foil.

Fig. 3 shows the normalized energy resolution versus the mean light output for the various cases. The curve shown is based on eq. (9)

$$\sigma_0^2 = \frac{1}{\bar{n}_{\text{eff}}} + \text{const.}$$

using $\bar{n}_{\text{eff}} \simeq 730/\text{GeV}$ for the reference module (table 1).

It is obvious that there is no need to polish the edges of the scintillator plates, resulting in drastically reduced cost. It has been checked that the unpolished edges of the scintillator plates do not deteriorate the homogeneity of light collection.

The effect of the leakage term eq. (4), can be seen from fig. 4, where σ_0 is plotted as a function of energy. At low energies, $E_0 \leq 1$ GeV, σ_0 is constant; at higher energies, σ_0 increases slightly, in quantitative agreement with eq. (14). The full line in fig. 4 shows the influence of the leakage term alone, as derived from a Monte-Carlo simulation of showers [8], in agreement with eq. (4). The

* Röhm GmbH, Darmstadt, FRG.

** Altulor, Tour Gan, 92082-Paris la Defense, France.

dotted line is a quadratic sum of the leakage term plus a constant $\bar{\sigma}_0 = 7\%$. Thus it seems that all contributions to σ_0 are well understood and are essentially in agreement with eq. (9).

4. Test results

In the following section, the performance of a system of "standard" modules is described.

Fig. 5 shows the mean pulse height as a function of the energy, for particles hitting the center of a module. As in all the following figures, results for energies below 380 MeV were obtained using a photon beam; high-energy points refer to incident electrons. Over two orders of magnitude in energy, the observed deviations from linearity are less than 15%. The slight deviation from linearity, which is observed at low energies, could be due to transition effects at the lead–scintillator boundaries [5,6]. In the present case, however, the observed effect is still within the limits of the systematic errors due to uncertainties in the pedestal subtraction, calibration of beam energies and of the tagging system, etc.

As already mentioned, fig. 4 illustrates the normalized energy resolution for central incidence on a counter module.

Even for photon energies as low as 70 MeV, the counter still provides a relative energy resolution of 27% r.m.s. (fig. 6) and is practically 100% efficient. A convenient definition for the lowest energy which can be detected reliably is given by the point where mean pulse height is three times the r.m.s. resolution, i.e. the energy where a single particle gives a 3 s.d. signal. In that sense, the shower counters provide a low energy cutoff of 45 MeV.

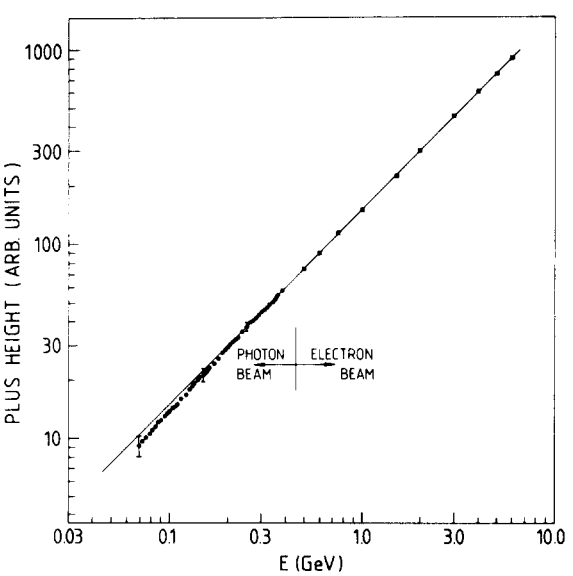

Fig. 5. Mean pulse height as a function of particle energy. Statistical errors are negligible; the error bars correspond to systematical errors at low energies.

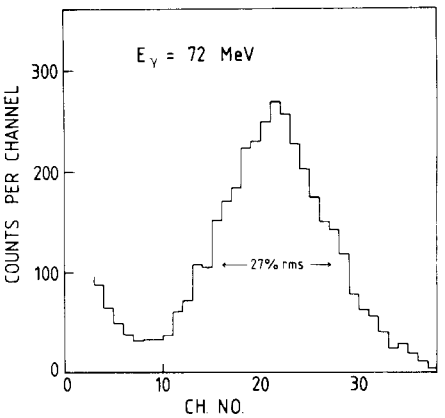

Fig. 6. Pulse-height distribution for 72 MeV-photons. The counts in channels below 10 are due to the soft-photon background in the tagged beam.

The results shown in figs. 4–6 were obtained using beams which hit a module at its center, perpendicular to its surface. In practice this is a very rare case and it is important that a shower counter provides good homogeneity over its whole surface. In the present design, there are two regions which may give rise to inhomogeneities: at three of the sides, a module is separated from its neighbours by 2 mm iron, plus 2 mm air due to tolerances in the dimensions of the scintillator plates and the steel housings. At the fourth side, the active areas of two modules are further separated by the two 5 mm thick wave-length shifter bars (fig. 7).

Figs. 8(a) and (b) show the normalized energy resolution and the mean pulse height measured in the counter

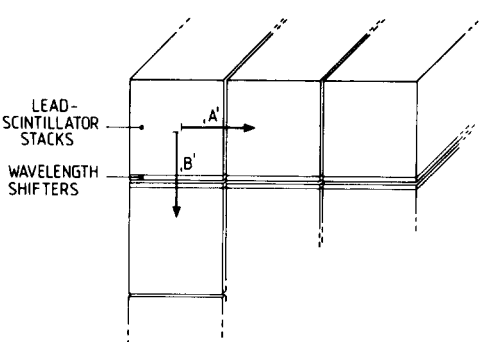

Fig. 7. Arrangement of counter modules. In order to investigate the influence of the gaps between the modules, the beam was scanned along lines "A" and "B".

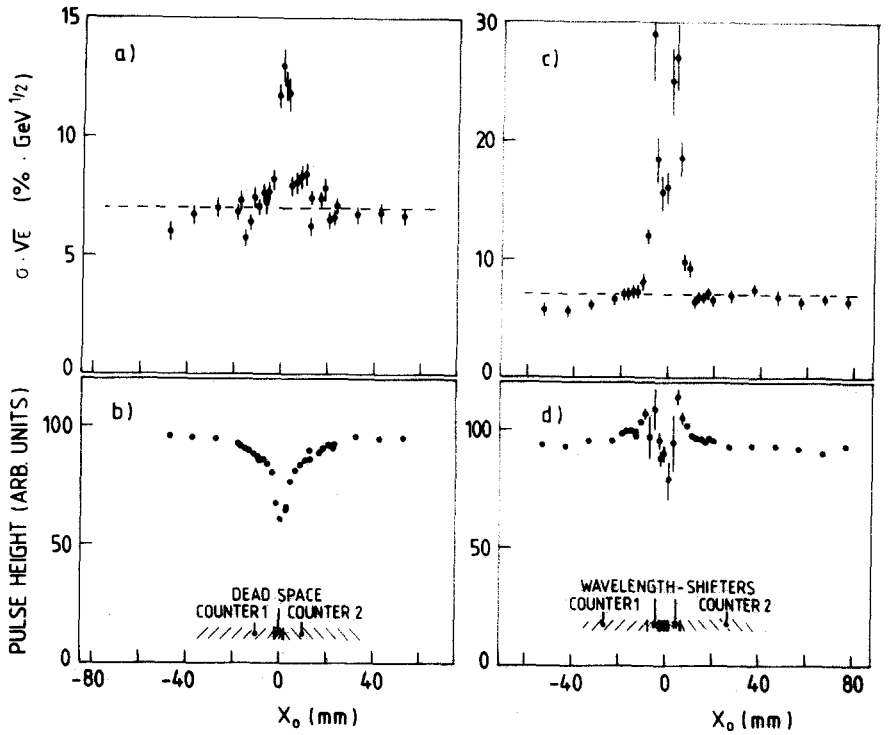

Fig. 8. Normalized energy resolution (a, c) and mean pulse height (b, d) as a function of the impact position x_0 of photons, along line "A" (a, b) or "B" (c, d) defined in fig. 7, measured at photon energies of 200–320 MeV, for perpendicular incidence. Dotted lines indicate the "standard" energy resolution $\sigma_0 = 7\%\ \mathrm{GeV}^{1/2}$.

array, as a function of the impact coordinate x_0 of the beam, which is moved along the line "A" in fig. 7. The direction of the beam is exactly perpendicular to the surface of the counter modules. When the beam hits the gap between the active area of the two modules, the visible energy decreases and the resolution worsens, as compared with the value $\sigma_0 \simeq 7\%\ \mathrm{GeV}^{1/2}$ indicated as a dotted line. The disturbance due to the gap diminishes at distances larger than ~ 10 mm from the boundary.

Figs. 8(c) and (d) show the corresponding quantities as a function of the position x_0 along the line "B" traversing the region occupied by the wave length shifters. The hole in the visible energy is less pronounced than in (b), since part of the effect is cancelled by Cherenkov-light produced by shower particles in the wave-length shifter and in the light guide. The large fluctuations associated with this component however drastically worsen the energy resolution of the system.

For non-perpendicular incidence of particles, these effects are much less pronounced, since in general only a small portion of shower is contained in the gap region. This is demonstrated by fig. 9, where the energy resolution measured for the worst case (impact position such that the shower maximum crosses the gap between two modules) is plotted for different angles of incidence. Fig. 9 proves that already at angles of 10° with respect to normal incidence no distortion due to the gap is seen. Averaging over the surface of a module and over possible angles of incidence up to 45° (corresponding to the geometry of solenoid detectors), about 90% of all photons observed in the calorimeter are detected with an

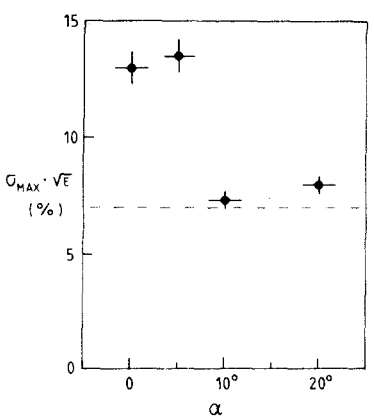

Fig. 9. Largest value of $\sigma E^{1/2}$ measured during a scan across the gap between two modules, as function of the angle α between the beam axis and the normal to the counter surface. α is oriented such that the shower axis intersects the gap region between two modules.

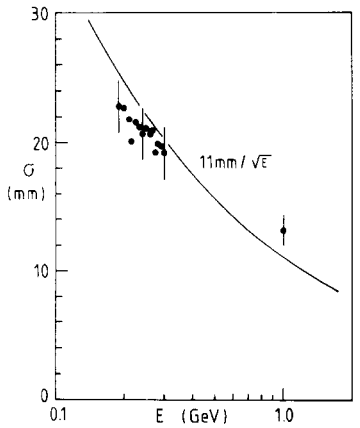

Fig. 10. The r.m.s.-deviation between the impact point and reconstructed coordinates, averaged over x_0 (see fig. 7), as a function of energy.

accuracy

$\sigma E^{1/2} \lesssim 10\%\ \mathrm{GeV}^{1/2}$.

Finally, fig. 10 shows the position resolution of the device for perpendicular incidence of particules, averaged over impact positions. The impact point of a photon can be reconstructed with an accuracy $\sigma \simeq (10\text{–}11\ \mathrm{mm})/E^{1/2}$ (E in GeV), which is slightly worse than that estimated from eq. (15).

We are indebted to Prof. G. Nöldeke for his interest in this test and for permission to use the BONN-Synchrotron. We acknowledge the valuable help of Drs. J. Arends, A. Hegerath and B. Mecking, who assisted during the setup of the test and who provided the photon tagging system. We are grateful to the operators of synchrotron at Bonn, P. Haas, J. Karthaus and K. Küffner, whose continuous effort allowed us to run the synchrotron at unusually low energies, thus enabling us to test the behaviour of shower counters at very low photon energies. We wish to thank the synchrotron group at DESY, and the mechanical workshops at Dortmund and at DESY for their support of this test. Finally, we thank Dr. J. Spengler for helpful comments and for his careful reading of this manuscript.

This work has been supported by the Bundesministerium für Forschung and Technologie.

References

[1] W.A. Shurcliff, J. Opt. Soc. Am. 41 (1951) 209; R.C. Garwin, Rev. Sci. Instr. 31 (1960) 1010; G. Keil, Nucl. Instr. and Meth. 87 (1970) 111; A. Barish et al., CALT 68-623 (1977); W. Selove et al., Nucl. Instr. and Meth. 161 (1979) 233.

[2] W.B. Atwood et al., SLAC-TN-76-7 (1976); V. Eckardt et al., MPI-PAE/Exp. El 70 (1978); V.K. Bharadway et al., Nucl. Instr. and Meth. 155 (1978) 411.

[3] W. Hofmann et al., Nucl. Instr. and Meth. 163 (1979) 77.

[4] E. Longo, I. Sestili, Nucl. Phys. 128 (1979) 283; R.K. Bock, T. Hansl-Kozanecka and T.P. Shah, CERN-EP/80-206 (1980).

[5] K. Pinkau, Phys. Rev. 139 (1965) 1548; C.J. Crannel et al., Phys. Rev. 182 (1969) 1435.

[6] C.J. Crannel, Phys. Rev. 182 (1969) 1141; and refs. therein.

[7] K. Greisen, Phys. Rev. 75 (1949) 1071.

[8] J. Engler et al., Nucl. Instr. and Meth. 120 (1974) 157; W. Hofmann, KFK-Ext. 3/74-10 (1974).

[9] U. Amaldi, Phys. Scripta 23 (1981) 409.